Laser System: Powerful XeCl* Laser - Dye Laser for Ecological Monitoring of the Atmosphere

Tatyana N. Kopylova*, Georgii V. Mayer*, Victor F. Tarasenko**, Rimma T. Kuznetsova*, Lyibov G. Samsonova*, Valerii A. Svetlichnyi*, Evgenii N. Tel'minov*, Sergei V. Mel'chenko**, Sergei E. Kunts**, Evgenii H. Baksht**, Alexei N. Panchenko**, Evgenii A.Andrushak***, Alexander L. Onitschenko***,

* Siberian Physical Technical Institute, Tomsk State University, 1, Novosobornaya sq., Tomsk, 634050, Russia

**High Current Electronics Institute, 4, Akademichesky ave., Tomsk, 634055, Russia

*** Scientific Research Institute of Space Equipment, 53, Aviamotornaya st., 111250, Moscow, Russia

ABSTRACT

The present paper reports the experimental results and design of the laser systems developed for lidar experiments. The laser systems with radiation energy of hundreds of millijouls at each of several wavelengths allow to detect NO_2 and SO_2 atmospheric impurities. At the moment the laser system: powerfull XeCl*-laser - dye laser is incorporated in a lidar developed at the Scientific Research Institute of Space Equipment (Moscow) for measurements of NO_2 content in the atmosphere.

Keywords: narrow-band laser radiation, dye, master oscillator, amplifier, output energy

1. INTRODUCTION

Laser monitoring of atmospheric impurities is currently one of the most pressing problems. The most widespread method of monitoring, differential absorption, is based on detection of light backscattered by the atmosphere at different distances from a probing laser. The laser should be capable of emitting two wavelengths (λ_{on} and λ_{off}), the first lying in the absorption band of an admixture under investigation (λ_{on}), and the other belonging to the region where the atmosphere is relatively transparent (λ_{off}). It is clear that the laser radiation spectral width at each wavelength should be relatively narrow (of the order of one tenth of angstrom). Moreover, a long distance lidar should feature high radiation intensity (of the order of hundreds of millijouls), because the scattered light intensity falls with a distance R more rapidly than R^2. The most perspective lidars allow one to detect several types of impurities with minimum change in the configuration of the laser system. However, the reported laser energy did not exceed several tens of millijouls, and thus the probe distance was limited. Thus, powerful laser systems providing wavelength tuning is necessary for the lidar development[1,2].

In the present report, XeCl-laser systems producing narrow band radiation at the wavelengths corresponding to the wings of XeCl* molecule transition ("weak" lines) with high signal-to-noise ratio (contrast) are described and studied both experimentally and theoretically. Besides, powerful XeCl - laser LIDA - 3M is described and tuned dye laser system pumped by the laser is reported. The laser systems produce high-quality beam with energy of hundreds of millijouls at wavelengths allowing to detect NO_2 and SO_2 atmospheric impurities.

2. EXPERIMENTAL APPARATUS AND RESULTS

2.1. XeCl* laser system with wavelength tuning

Two-stage laser system was developed on the base of two LIDA-T discharge lasers used us a master oscillator (MO) and an amplifier (A). The lasers produce output energy of 0.5 J in 50 ns pulse (FWHM) in free-running regime[3]. Therewith the ratio of the laser intensities on different transitions were $I_{0\text{-}0}:I_{0\text{-}1}:I_{0\text{-}2}:I_{0\text{-}3}$ = 2.5:50:20:1 ($E_{0\text{-}0}$ = 14 mJ; $E_{0\text{-}1}$ = 310 mJ; $E_{0\text{-}2}$ = 110 mJ; $E_{0\text{-}3}$ = 6 mJ). Note, that the ratio was not constant and changed with the pumping power and the gas mixture composition. For example, the ratio $I_{0\text{-}0}:I_{0\text{-}1}$ was increased until 1:8 when Xe content in the gas mixture exceeded its optimal

SPIE Vol. 3983 • 0277-786X/99/$10.00

value (see Fig.1)[4]. This effect was used to tune the laser system on the "weak" lines of XeCl*-molecule transitions. Then single-pass amplifier operating in the near-saturation mode was used to obtain high quality radiation at this line. For this purpose it was important to have a powerful beam from the MO (up to 30 mJ) and to use whole active volume of the LIDA-T amplifier. That is why the resonator similar to that described in[5] was used (see Fig.2): the 1200 grating GR operated in the first diffraction order in the autocollimation mode; lenses L1 (F=2 m) and L2 (F=10 cm) together with the gap G formed a spatial filter for selection of transverse modes; plane mirror M provided feed back.

This resonator with good optical quality had high level of mode selection and allowed us to use about 60% of the active volume. So with the gap of 100 μm the resonator quality at selected line was the same as in the case of a plane-parallel resonator used in the free-running regime. The output energy of the MO in this case was 30 mJ or 60 mJ on the "weak" or "strong" lines. The line width, divergence and pulse duration were 0.04 nm, 10^{-4} radian and 40 ns (FWHM), respectively. The contrast calculated as the ratio of a power at the selected wavelength and the sum of powers at three other lines:

$$K = P_{0\text{-}0} / (P_{0\text{-}1}+P_{0\text{-}2}+P_{0\text{-}3}) \text{ (for the 0-0 line)}$$

exceeded 100. In the process of amplification, any kind of feed back for a wide-band spontaneous noise had to be inhibited. The quartz plate M was used as an output mirror and the line narrowing results in decrease of the grating reflection coefficient but the cavity quality could be improved by increasing the output mirror M reflection coefficient. The powers P_i were calculated based on the equations of beam formation in a generator in the presence of two waves [6]:

$$dI^+/dz = -\alpha I^+ + g_0 I^+ / (1+ I^+ + I^-) \qquad (1)$$

$$dI^-/dz = -\alpha I^- + g_0 I^- / (1+ I^+ + I^-) \qquad (2)$$

where I^-, I^+ are the intensities of waves propagating along the optical axis z in the opposite directions normalized to the saturation intensity I_S; g_0 is the small signal gain; α is the unsaturated absorption coefficient. This calculation indicates that the active medium parameters should satisfy some requirements to provide high contrast on the "weak" transitions (see Fig.3). The contrast is low if the gain coefficient in the active medium is low or high (the laser active length is 60 cm). It was found experimentally that parameters of the LIDA-T output at the 0-0 transition (λ=307.7 nm) are as follows: g_0 = 0.054 cm^{-1}, α = 0.012 cm^{-1}, I_S = 1.4 MW/cm^2. The g_0 value is close to but lower than optimal gain for the MO active medium. So we can expect to improve output energy on the "weak" lines by a factor of 1.5 - 1.7 without any reducing in the contras.

As it is seen from Fig.4, the regime of single-pass amplification with input energy of 30 mJ is close to the saturation one and the contrast in the amplifier output exceeds 100 with output energy of 210 mJ. Narrowing line to 0.01 nm via the gap reduction results in tenfold fall of the output energy. As a result the contrast is reduced to 3 - 40. However it can be restored by the choice of spatial geometry of beam propagation through the amplifier active medium. So, if the beam has a spherical wave front with the center at the point located in 30 cm before the active medium, the output contrast will again exceed 100. It is the consequence of the amplifier saturation due power density increase. But it is also clear that the output energy in this case decreases because the part of the active volume is not used. The above conditions were simulated basing on the equation of light beam propagation through an active medium [6]:

$$(g_0 -\alpha)\times L = \ln(I(L)/I(0)) - g_0/\alpha\times\ln(\{g_0-\alpha\ (1+I(L))\}/\{g_0-\alpha\ (1+I(0))\}) \qquad (3)$$

The calculations showed that one can to chose geometry of the amplified beam propagation providing maximal contrast with minor decrease of the output even for relatively low input energy (see Table 1). The effect of mixture composition and pumping power was insignificant in the single-pass regime.

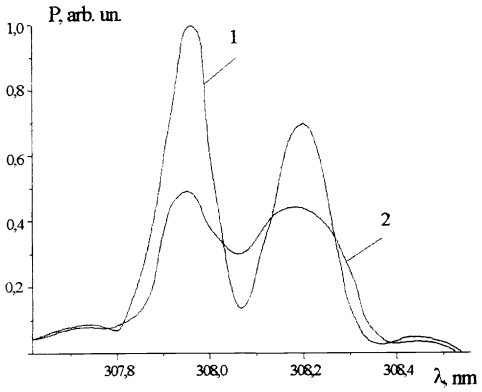

Fig.1. Output spectrum of the LIDA-T laser obtained in optimal gas mixture (1) an in mixture with doubled Xe content (2).

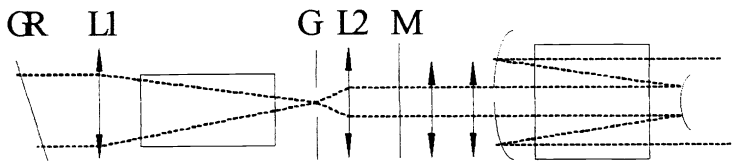

Fig.2.
Optical scheme of XeCl* laser system with wavelength tuning. GR is grating worked in an autocollimation regime, L1 and L2 are lenses, M is mirror, G is the spatial selection gap.

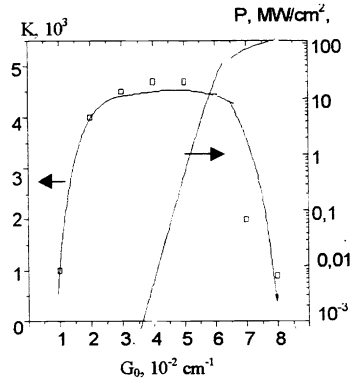

Fig.3. Calculated output energy and contrast of laser system versus active medium gain coefficient. Active medium length is 60 cm.

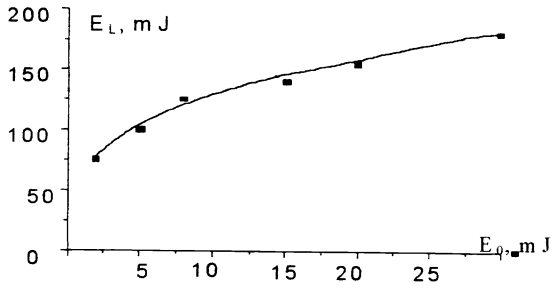

Fig.4. The LIDA-T amplifier output power as a function of input power obtained experimentally.

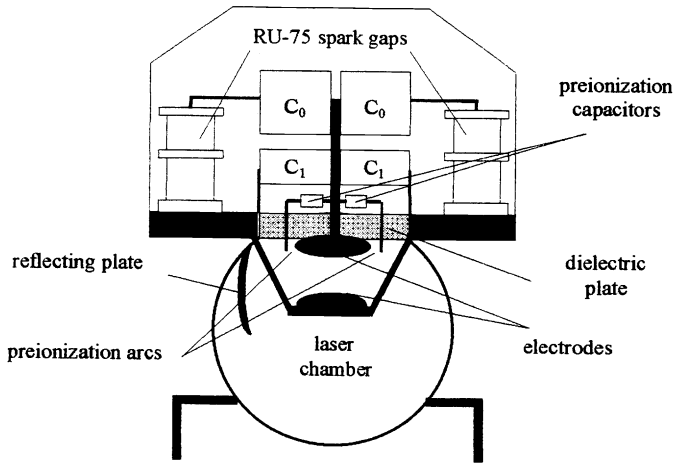

Fig.5. The LIDA - 3M laser schematic diagram. C_0 and C_1 are storage and peaking capacitors, respectively.

Table 1.Radiation energy and signal to noise ratio at the amplifier output versus input energy and spatial geometry of amplified beam.

Type of	E_0= 0.3 mJ		E_0=3 mJ		E_0=15 mJ		E_0=30 mJ	
the beam	E_L, mJ	K	E_L, mJ	K	E_L, mJ	K	E_L, mJ	K
1	4	4	30	23	115	51	183	66
2	3	18	20	51	60	79	90	94
3	3.5	13	27	43	82	75	120	98
4	3	8	18	40	55	71	84	92

E_0 - input energy, E_L - output energy, K - signal/noise ratio. 1- parallel beam, 2 - beam focused at the beginning of the active medium, 3 - beam focused at 30 cm before the active medium edge, 4 - beam focused at the middle of the active medium.

The injection locking regime was also tested in our experiments on amplification of laser radiation on the "weak" lines. Threshold power in this regime was 20 W/cm^2. But due to self-excitation on the "strong" lines contrast at the amplifier output does not exceed 1. However in this case the gas mixture composition has found to play an important role. For instance, the contrast of 20 and output energy of 150 mJ were obtained in gas mixture containing 40 Torr of Xe (its twofold optimal value) and total pressure of 4 atm. Other necessary conditions consist in decrease of the charging voltage and the use of low magnification coefficient of the resonator (M = 3). Maximal radiation energy obtained in this regime (300 mJ) was close to that obtained when the amplifier operates without injection. However, in this case the contrast did not exceed 3 - 5. Notice that the contrast increases with the distance from the amplifier due to different divergence of the signal and noise beams. According to our estimations the contrast will exceed 100 at the distance of 100 m.

2.2. Powerful XeCl - laser LIDA - 3M

For pumping dye lasers powerful XeCl - laser LIDA-3M was developed. The laser schematic is shown in Fig.5. The laser electrical circuit includes storage and peaking capacitors with capacitances C_0 = 60 - 120 nF and C_1 = (0 -0,8)C_0, respectively. Industrial low-pressure RU-75 spark gaps are used as switches. The laser electrodes are placed on one side of a dielectric plate while the capacitors are located on its other side. Arcs placed along one of the electrodes provided gas preionization during pulsed charging of capacitors C_{pr}. A concave metal plate located on the side of the laser gap improves pulse repetition rate of the laser. The use of the plate increases average output power by a factor of 1,5. The laser operates with pulse repetition rate up to 5 Hz with average output power up to 3 W.

The LIDA-3M laser pulse duration depends on the ratio C_1/C_0. Output pulses with full duration of 300 ns are obtained at C_1 = 0 (in this case C_{pr} = 3.5 nF serve as peaking capacitors). Laser energy over 1 J with an efficiency up to 3% was obtained in this pumping regime.When C_1 was increased to 0,8C_0 laser pulses with 45-55 ns in duration (FWHM) and 15-20 ns rise-time were obtained. The laser energy and efficiency versus charging voltage of storage capacitors are plotted in Fig.6. Output energy of 1.2 J with peak power of 20 MW and efficiency up to 2% were easily obtained. These pulses were found to be optimal for excitation of dye laser system.

2.3. MZhL-03 dye laser system

Schematic diagram of the MZhL-03 dye laser system producing narrow-band tuned radiation is shown in Fig.7. The laser system includes a master oscillator (MO), preamplifier (PA) and amplifier (A). Pumping energy E_{XeCl} is distributed over these elements in the ratio 0,15:0,3:0,55. The MO cavity is formed by an output mirror and two gratings one of which operates in the mode of grazing beam incidence while the other is used in the Littrov scheme. Usually MO optical schemes using a beam spreaders and multiprism cavities allowed to convert XeCl - laser radiation with an energy lower 0,5 J into narrow-band dye radiation with an divergence about 3 mRad[8].

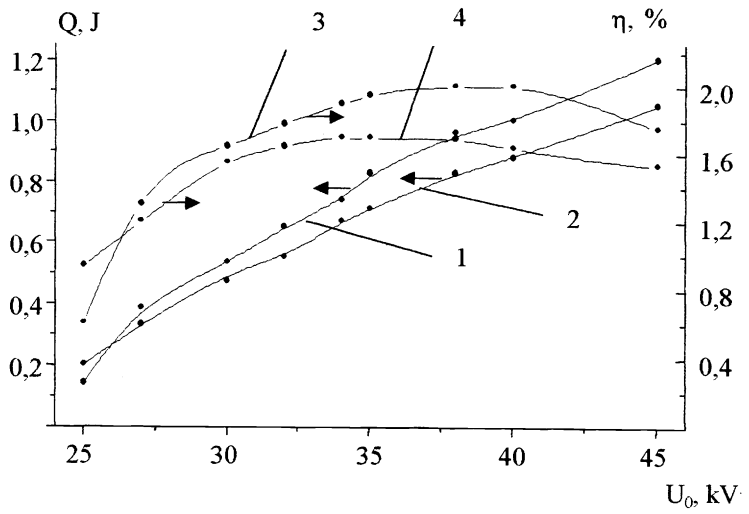

Fig.6. Output energy (1, 2) and efficiency (3, 4) of the LIDA-3M laser as a function of charging voltage of storage capacitors. $C_1 = 0{,}8\ C_0$. Gas mixture of the Xe:HCl = 18:3 Torr composition at p=3 atm (2, 4) and p=3,5 atm (1, 3) is used.

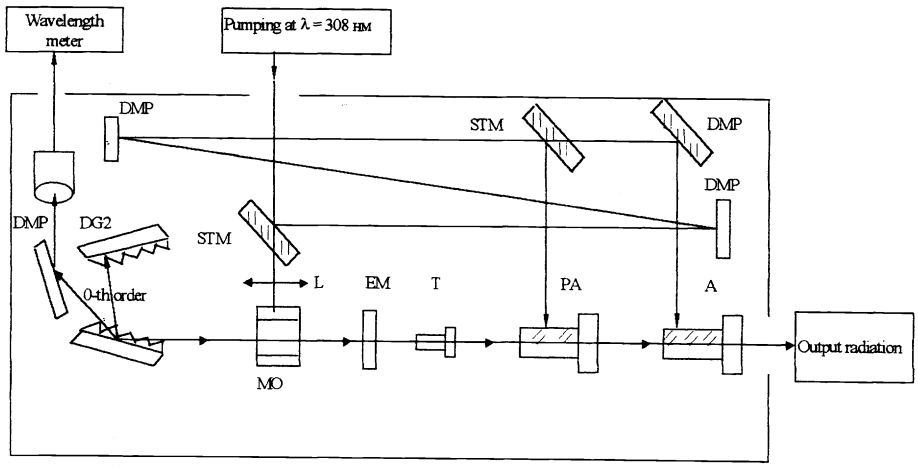

Fig.7. Block diagram of the MZhL dye laser system. MO, PA, A are the master oscillator, preamplifier, amplifier, respectively, STM are semitransparent mirrors, DMP are total reflectors, DG1-2 are diffraction gratings, EM is the MO output mirror, T is a telescope, L is a cylindrical lens.

The optical scheme used in the MZhL laser system allows us to convert up to 1,5 J of XeCl radiation into high-quality visible light with the signal to noise ratio over 1000, near-diffraction divergence (up to 53% of the MO output is propagated in a solid angle of 1,4 mRad) and band-width $\Delta\lambda \leq 0{,}01$ nm. The PA and A cells made as prisms of total internal reflection (TIR) do not require focusing of pumping radiation and can convert up to 1.5 J without their damage (in this case specific input power does not exceed 4 MW/cm^2).

Coumarin -2 solution in ethanol is used as a dye active medium. The dye concentration was optimized for each element. Besides a regenerating system[9] significantly improves the active medium life-time.

As a rule, the higher is XeCl laser energy the longer is the laser pulse duration, especially its rise-time. Therefore output parameters of the MZhL laser were studied at different pumping pulse duration. The dye laser conversion efficiency versus input energy obtained for pumping pulse duration τ_p = 40, 55 and 75 ns is shown in Fig.8. It is seen that the efficiency decreases at longer pumping pulses. We explain that effect not by the dye photophysical properties since the efficiency does not change when the MO is equipped with a nonselective cavity, but by a mismatching of the delay time of the MZhL - laser (the time interval between the onset of lasing in the MO and the instant a pumping pulse falls on the PA and A) designed for XeCl pulses with τ_p = 40-50 ns and rise-time of 10-15 ns. The delay time is determined by the MO lasing threshold. Therewith the shorter is the rise-time, the earlier the threshold is reached.

The ratio of the MO pulse duration to τ_p = 40 ns proportional to the MO efficiency (curve 1) and the MO pulse rise-time for τ_p = 40 ns (curve 2) and τ_p = 75 ns (curve 3) versus specific input power are shown in Fig.9. One can see that curves 1 and 2 saturate at P≥2 MW/cm^2 which corresponds to the input energy of 0,2 J. This means that further increase of the energy does not change the MO efficiency and its pulse shape. Thus, the MO operates in stable regime at τ_p = 40 ns if the pumping energy is over 0,2 J. Curve 3 obtained for τ_p = 75 ns saturates only at W approaching 3 mW/cm^2 which corresponds to the pumping energy of 0,6 J. Thus, stable operation of the dye system pumped by a XeCl* pulse with duration of 75 ns and rise-time of 30 ns is achieved at the pumping energy over 0,6 J/cm^2 and increasing the MO efficiency requires longer delay time and changes in its optical scheme.

In addition to the temporal parameters of a XeCl laser pulse input beam aperture and divergence are of great importance. The PA and A cells have input apertures of 48×16 mm^2. Therewith pumping energy entering the PA and A is maximal if the beam aperture and divergence are equal to 38 × 14 mm^2 and 3×1,5 mRad, respectively. Increase of the aperture or divergence results in higher losses of the pumping energy and decrease the MZhL system efficiency. This effect is especially pronounced when pumping energy of the amplifier E^A_p becomes deficient at increased beam divergence. The divergence increase was simulated by decreasing E^A_p. The results obtained are listed in Table 2. It is seen that for τ_p= 40 ns and E_{XeCl} =0,39 J two-fold decrease of E^A_p results in the fall of the MZHL laser system efficiency from 13% to 7% while at optimal distribution of the pumping energy over the laser elements the same reduction of E^A_p gives the efficiency fall only from 13% to 11,8% .

Table. 2. Total pumping energy of the MZHL-3 dye system E_p^{XeCl}, input energy at MO E_p^{MO}, PA E_p^{PA} and A E_p^{A} and the dye system efficiency. The pumping pulse duration is τ_p=40 ns.

E_p^{XeCl}, mJ	E_p^{MO}, mJ	E_p^{PA}, mJ	E_p^{A}, mJ	η, %
390	59	117	215	13
195	28,5	58	108	7,8
283	42,5	85	156	11,8
283	59	117	107	7

MZhL-03 laser pumping by means LIDA-3M laser with parameters mentioned above: E_{las}=550-700 mJ,τ_{FWHM}=55 ns with rising slope not exceeded 20 ns and pumping beam dimensions of 38×13 mm^2, allows to obtain the conversion efficiency up to 13 % and generation energy at 448 nm of 87 mJ with the line width $\lambda_{las} \leq 0{,}01$ nm (Table 3).

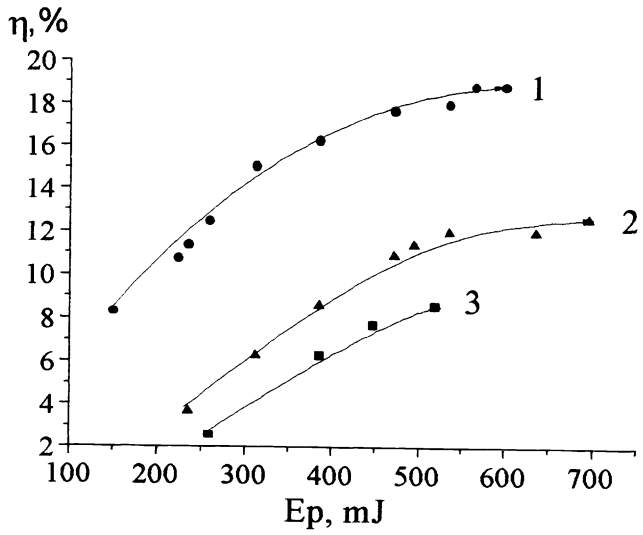

Fig.8. Efficiency of the MZHL-03 laser system versus energy of XeCl laser with pulse duration of 40 ns (1), 55 ns (2) and 75 ns (3).

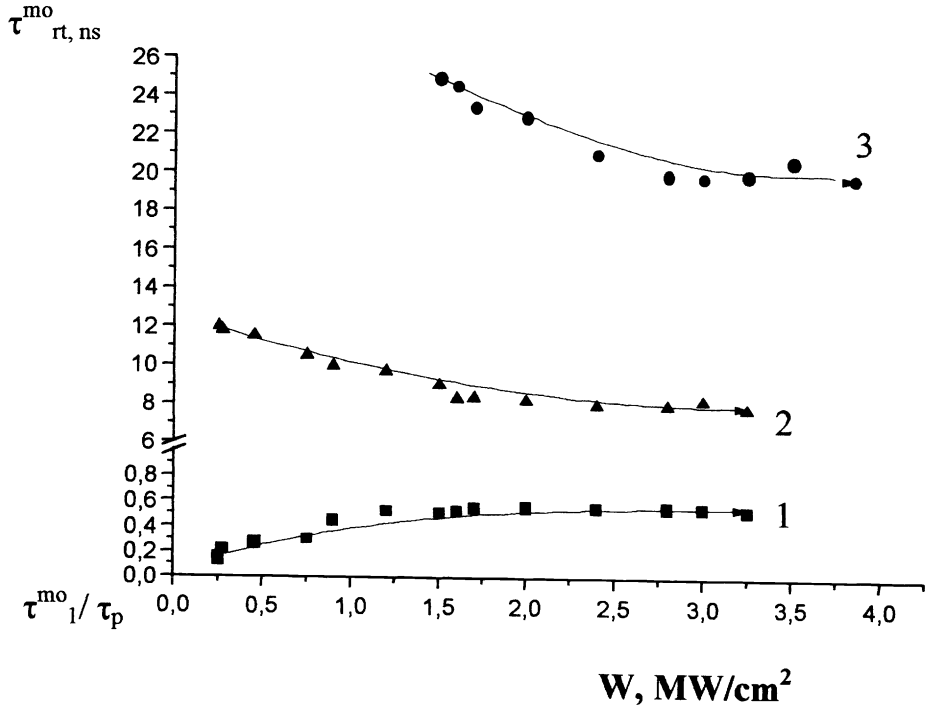

Fig.9. Ratio of the MO pulse duration to that of pumping pulse τ^{mo}_{l}/τ_p (1) and rise-time of the master oscillator pulse τ^{mo}_{rt} (2,3) versus specific input power on the MO obtained at τ_p=40 ns (1,2) and , τ_p=75 ns (3).

Table 3.Characteristics of laser system: LIDA-3M – MZHL-03

E_p,mJ	τ_{FWHM}^p, ns	S_p, mm^2	E_{las}, mJ	η, %
550	50	38×13	70.3	12.8
660	55	38×13	78	11.8
700	55	38×13	87	12.4

Thus, the potentialities of the MZhL-0,3 laser system were studied. It was found that the dye system maximal efficiency of 18.8% is achieved at τ_p = 40 ns and E_{XeCl} >0,5 J when XeCl* laser beam divergence is 3×1,5 mRad and its aperture is 38×14 mm^2. The efficiency falls to 13% at τ_p = 55 ns and E_{XeCl} >0,6 J, the beam divergence and aperture being the same.

2.4. Lidar radiation sources

The sources of lidar radiation includes two laser channels, each consisting of the following systems: XeCl*- laser oscillator-amplifier (on the base of the LIDA-T lasers) or LIDA-3M laser - the MZhL-03 dye system. When monitoring SO_2 impurity, only the oscillator-amplifier laser systems are operated. The wavelength in the first channel is λ_{on} =308,45 nm, and in the second one - λ_{off}=307,7 nm. The radiation energy is up to 0,25 J per pulse and the line width is 0,01-0,03 nm, the contrast measured with respect to the broadband noise is over 50 in each channel.

In the NO_2 monitoring mode the LIDA-3M laser pump the MZhL-03 dye system. The first channel is tuned to λ_{on} =446,9 nm, and the other one to λ_{off}=448,2 nm. The radiation energy and the line width in each channel are ~0,15 J and 0,01 nm, respectively. The lidar operates at a pulse repetition rate up to 5 Hz and the channels are synchronized to provide a time delay of 10 ms for each channel.

The further step in development of lidar system was setting of optical-mechanical wavelength switch in the MZhL-03 block. That makes possible to get in one channel the radiation with two wavelength (λ=446.9 and 448.2 nm) switched by turn. It simplifies the wavelength commutation in the two-channels generator and eventually leads to the general improvement of lidar system.

3. CONCLUSION

The experimental design of the laser systems producing a radiation energy of hundreds of millijouls at wavelengths allowing to detect NO_2 and SO_2 atmospheric impurities is described.

In the NO_2 monitoring mode the LIDA-3M - laser pumps the MZhL-03 dye system. The first channel is tuned to the wavelength λ_{on} = 446,9 nm and the other one is tuned to λ_{off} = 448,2 nm. The dye system provides the efficiency relatively to XeCl* - pumping up to 18%. The line bandwidth in each channel is 0,01 nm. The lasers operate at a pulse repetition rate up to 5 Hz and are synchronized to provide a time delay of 10 ms for each channel. At the moment the laser system: powerfull XeCl*-laser - dye laser is incorporated in a lidar developed at the Scientific Research Institute of Space Equipment where measurements of NO_2 content in the air under industrial areas of Moscow have been carried out.

In the SO_2 monitoring mode the XeCl* - laser system operates in the regime of amplification. The first channel is tuned to the wavelength λ_{on} = 308,45 nm, the other one is tuned to λ_{off} = 307,7 nm. The output energy was up to 250 mJ with the line bandwidth of 0,01 - 0,03 nm. The system is planned to be used in the lidar at the Scientific Research Institute of Space Equipment (Moscow).

4. REFERENCES

1. K.S.Gochelashvili, M.V.Kabanov, V.B.Kaul, T.N.Kopylova, G.V.Maier, S.V.Mel'chenko, A.N.Panchenko, A.M.Prokhorov., V.F.Tarasenko, E.N.Tel'minov "Model Laser System for Ecological Lidar." *Laser Physics.* **2**, No.5, 802-804. 1992.

2. V.Ya. Aryukhov, I.V.Sokolova, T.N.Kopylova, G.V.Mayer, V.F.Tarasenko, and V.D.Kuznetsov, "Development and design of powerful excimer laser-pumped dye lasers", Proc. Int. Conf. on LASERS'94, Quebec, Canada, 208-215. 1994.

3. V.S.Verkhovsky, M.I.Lomaev, S.V.Mel'chenko, A.N.Panchenko, V.F.Tarasenko "Control of temporal, spatial and energy parameters of the XeCl laser radiation" *Kvant. Electron.*, **18**, No.11, 1279-1285. 1991.

4. V.B.Kaul, S.E.Kunts, S.V.Mel'chenko " Saturation intensity and output radiation spectra of XeCl-laser." *ibid.*, **22**, No.6, 555-558. 1995.

5. M.S.Dgidgoev, I.A.Kudinov, V.T.Platonenko, E.V.Slobodchikov, M.K.Shayachmetova "Regenerative amplification of radiation in excimer XeCl-laser" *ibid.*, **17**, No.7, 697-703. 1990.

6. N.V.Karlov *"Lekzii po kvantovoy electronike (Lectures on Quantum Electronics)"*, Moscow: Nauka, (1983).
7. V.Yu.Baranov, V.M.Borisov, Yu.Yu.Stepanov *"Electrorazryadnye eksimernye lasery na galogenidach inertnych gasov (Electrodischarge excimer lasers on rare gases halides)"* Moscow: Energoatomizdat. 1988.

8. S.S.Anufric, S.A.Kartazaeva, A.F.Kurlovich, et.al. Izvestia Akademii Nauk BSSR, No.6, 10-13. 1989.
9. S.M.Vovk, V.M.Galkin, T.N.Kopylova, et.al. Russian Patent No. 2029424, H01S/213 published in Bulletin "Discoveries, inventions and industrial models", No.5. 1995.